14

POWER/DATA TELEMETRY TECHNIQUES FOR IMPLANTS OR WEARABLE SYSTEMS

ANIL K. RAMRAKHYANI AND GIANLUCA LAZZI

Department of Electrical and Computer Engineering, University of Utah, Salt Lake City, UT, USA

14.1 INTRODUCTION

With the advancement of microfabrication technology for low power and multi-functional devices (i.e., biosensors and neural stimulators), and their usage in the proximity of biological media, numerous medical devices and wearable electronics have been developed [1–5]. For each in-body (implant) and/or on-body (wearable) system, a stable power source and reliable communication data channel are key design requirements. While the design of the implanted device presents unique challenges such as small dimensions (1–2 cm), low power (1–100 mW), and high longevity (7–10 years), wearable electronics must be lightweight, and require multi-functionality and network connectivity with a standard wireless system (i.e., WiFi, Bluetooth). In the last decade, significant research has been devoted to create small, energy efficient implants that can be used to treat deafness (using cochlear implants), blindness (using retinal prostheses), pain management (using spinal cord stimulators), and Parkinson's disease (using deep brain stimulators). Wearable technologies have focused more on the choices that individuals can make in this digital age to access personal data (using biosensors) and information over the internet. With the vision of better information connectivity, multiple non-invasive devices such as Google Glass (for information

Electromagnetics of Body-Area Networks: Antennas, Propagation, and RF Systems, First Edition.
Edited by Douglas H. Werner and Zhi Hao Jiang.

access) [6], Apple Watch (for heart rate monitoring and information access) [3], and Fitbit (to create personal health log) [7] were developed.

For both implantable and wearable devices, specifications of the power and data telemetry need to be identified based on the underlying applications. However, few general methods and technologies have been developed to ease the constraints of these systems. For example, multiple wireless power transfer (WPT) methods (i.e., electromagnetic, acoustic) were proposed to create batteryless implants, achieving a small form factor. Similarly, to create a self-powered system, energy harvesting technologies (i.e., solar, biofuel, electromagnetic) have been developed. Some of these designs include life supporting devices (i.e., pacemaker, artificial heart), and therefore require a reliable data link for the regular monitoring of the device. Moreover, prosthetic devices such as retinal and cochlear implants require a stable (low error per packet) data link over which stimulation patterns can be transmitted in real time for the desired operation of the implant. For wearable electronics, the key requirement of the communication channel includes the use of standard protocol to achieve low power and a high data rate over a long (1–10 m) operating range.

In the following sections, different powering mechanisms and energy harvesting devices are discussed, including applications and their respective limitations. The data links for the wearable or implanted devices are categorized based on the use of low frequency propriety protocols versus the high frequency standard protocols. Moreover, two design examples are presented to discuss the implementation of a leading implanted retinal prosthesis and a wearable electronics based on body area network (BAN).

14.2 POWERING OF IMPLANTS AND WEARABLE SYSTEMS

In recent years, multiple powering techniques have been adopted to operate implanted and wearable devices. Even if traditional power storage units such as on-site battery remain the key source of power, multiple alternatives such as wireless power and energy harvesting devices were used to achieve long-term device operation of the miniaturized implanted systems. Similar approaches, which lead to larger discharging/replacement time of the battery, were taken for wearable electronics. Selection of specific powering mechanisms, such as an external power source (i.e., battery) versus the energy harvesting devices depend on the energy and size requirements of the underlying system. Figure 14.1 provides a detailed categorization of leading powering mechanisms. The following sections discuss different methods for powering implanted and wearable devices using non-regenerative and regenerative energy sources.

14.2.1 Non-Regenerative Power Sources

With the advancement of micro- and nano-electronics technologies, it is possible to accommodate complex and computationally intensive designs (i.e., microprocessor, image processor) while achieving the size constraints of the implantable and

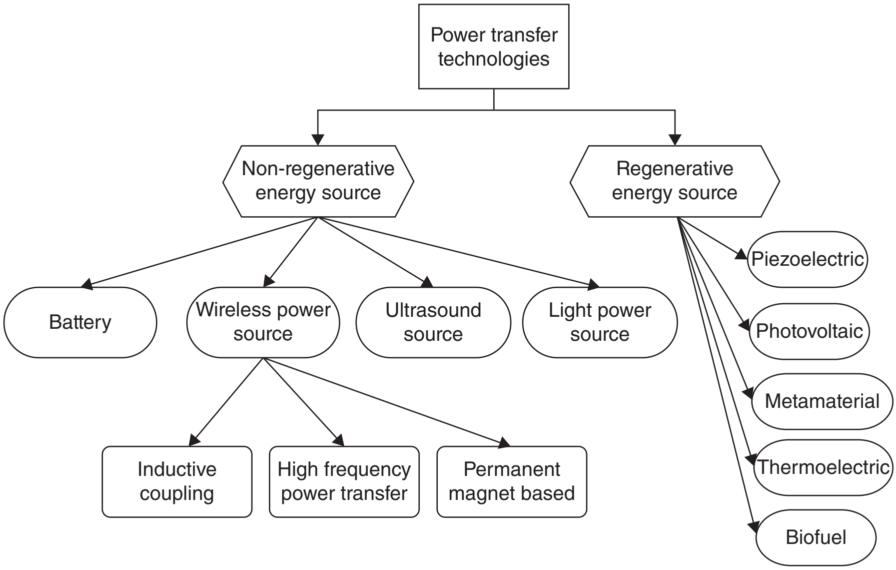

FIGURE 14.1 Different powering techniques for implanted and wearable devices. Multiple non-regenerative and regenerative methods can be chosen based on the underlying application's specifications.

wearable devices. Traditionally, dedicated power sources (non-regenerative) were used for systems with power requirements of the order of tens of milliwatts [8–10]. For many designs, especially for implanted devices, the moderate energy density of the implantable batteries restricts the device longevity. Therefore, many designs require alternate power transfer techniques from the dedicated external (outside the body) power source to the implanted electronics [11–13]. In the following sections, some of the dominant powering mechanisms are discussed for wearable as well as implanted systems.

14.2.1.1 On-Site Battery Operated Devices For wearable electronics, dedicated weight, volume, and form factor for the battery are significantly limited. With the growing demand for high energy density batteries and flexible form factors, the research community has utilized different materials [14] and developed new fabrication technologies [15]. Li-ion-based coin or polymer batteries dominate the consumer electronics market due to their wide availability in different form factors. Meanwhile, some research was conducted to achieve a Li-ion-based flexible battery [15]. To achieve paper-like flexibility, lightweight carbon nanotubes (CNT) were deposited on commercially available paper to create thin film current collectors (anode and cathode). This design achieved high energy density per unit mass (108 mAh/g) while maintaining its high flexibility and light weight, making it useful for powering wearable biometric gadgets used during sports activities. For most wearable electronics, the device lifetime is much longer than the battery discharge time. Therefore, rechargeable batteries with a large number of charge cycles (~1000–2000) and moderate discharge periods (~1–2 days) were used to achieve a battery lifespan of over 5 years.

For implantable devices, the energy capacity of the battery depends on the targeted lifetime and average power requirement of the implant. The battery is hermetically sealed inside a titanium case to meet the safety guidelines for medical devices. Spinal cord stimulators [16] or pacemakers [17] are examples of successful medical devices that use implanted batteries to achieve a device lifetime of 7–10 years. For some designs, rechargeable batteries, along with WPT capability, are used to reduce the dimensions of the implanted battery.

14.2.1.2 Wirelessly Powered Devices Using Electromagnetic Fields In the last decade, WPT using electromagnetic fields became the gold standard for contactless energy transfer between the external power source (i.e., battery) and the implanted electronics. For these systems, the efficiency of the power transfer depends on the operating frequency, operating distance, and the dimensions of the external and implant coils (or antennas). Similar to implanted devices, multiple wearable systems also integrate passive radio frequency identification (RFID) tags to achieve keyless entry and contactless payment options. In all these designs, the interrogator device (connected to a dedicated power source) generates the power and/or data signal and seeks for the transponder's (implant or wearable RFID) response. Depending on the power requirement of the transponder (implant or RFID tag) and the size constraint of the antenna or coil, different methods were considered. The following sections describe three methods based on the operating frequency and electromagnetic field source.

14.2.1.2.1 Inductive Coupling Inductive coupling-based WPT systems are typically preferred for designs in which the magnetic coil's dimensions and operating distance are much smaller than the operating wavelength. For most medical devices, operating distances between the external and implant coils range from 5 mm to 30 mm [1, 8]. Typically, the operating frequency of the design is kept below 20 MHz to maintain the absorbed electromagnetic energy in the tissue below the regulatory limits [20]. Depending on the number of coils used for the power transfer, the system can be characterized as either a two-coil [21, 18] or a multi-coil design [19, 22]. Figure 14.2 shows the block diagram of two-coil and multi-coil WPT systems. For both system types, the external coil generates the time-varying magnetic field, which couples with the implanted coil for the power transfer. Due to the evanescent nature of the magnetic field, the operating range of the inductive link is generally limited to only a few centimeters. Compared to the two-coil design, the multi-coil design is relatively new [19] and has shown significant advantages, achieving higher power transfer efficiency, tunable induced voltage at the implant, wider frequency bandwidth for the data communication, and lower susceptibility in system performance during the coils' misalignment [23]. Moreover, it was shown that using a multi-coil inductive link system, the absorbed energy in tissue [24] and the unintentional radiated field [25] can be significantly reduced compared to its two-coil alternative. Depending on

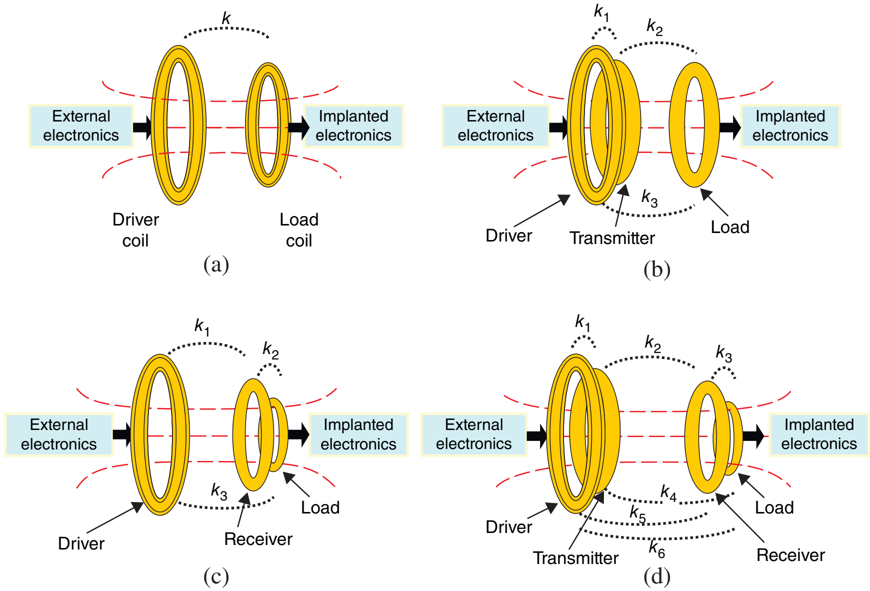

FIGURE 14.2 Two-coil and multi-coil wireless power transfer (WPT) system with different magnetic coupling between the coils. (a) Block diagram of the two-coil inductive link with the driver (external) and the load (implant) coil based on [18]. *Source:* Qusba et al. 2014 [18]. Reproduced with permission of IEEE. Block diagram of the three-coil WPT system with dual coils at (b) the external and (c) the implanted unit. (d) Four-coil WPT design with dual coils at the external and the implanted unit. *Source:* RamRakhyani et al. 2011 [22]. Reproduced with permission of IEEE. Compared to two-coil design, multi-coil WPT system achieves desired system's performance (efficiency, voltage gain, frequency bandwidth) by tuning vast design variables ($L_{1–4,}$ $k_{1–6}$).

the operating conditions, power transfer efficiency between 20% and 40% can be achieved over the inductive link. Therefore, this approach is quite suitable for high values of power transfer (100–300 mW) to the implant.

14.2.1.2.2 High Frequency Power Transfer High frequency WPT is a relatively new technique for operating low power (100–500 mW) and millimeter-size (2–4 mm in diameter) implants over mid-range (30–50 mm) coil separation [26, 27]. Due to low power transfer efficiency of the link (0.1–0.5%), this technique was primarily utilized for implantable sensors or low power neural stimulators [26]. Compared to an inductive link, high frequency WPT systems are operated over the frequency range of 1–2 GHz. The power generated by the external source is limited to 1–2 W to meet the specific absorption rate (SAR) and radiation guidelines of the federal regulatory agencies (Federal Communications Commission in the USA, International Electrotechnical Commission in the European Union). Figure 14.3 provides the block diagram of the high frequency wireless power link. Similar to an inductive link, the source generates an electromagnetic field near the implant site. Due to the

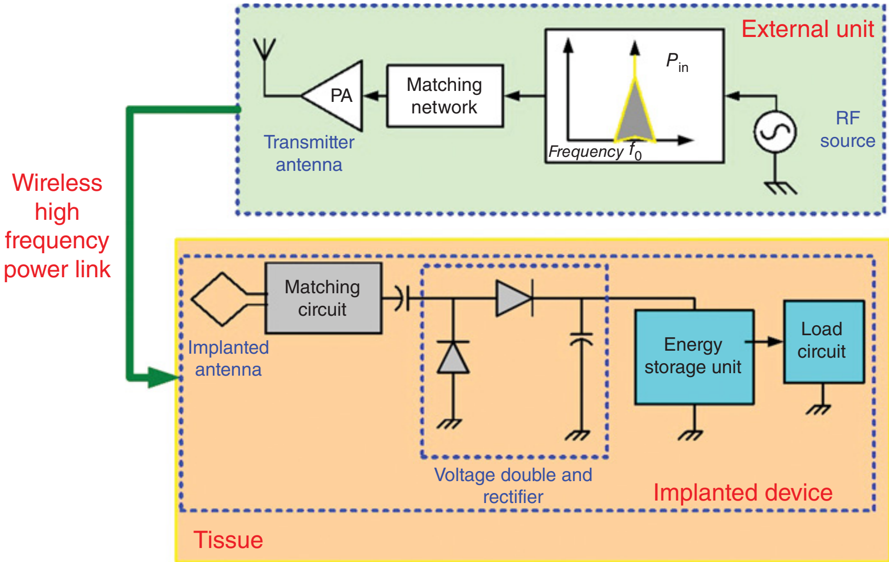

FIGURE 14.3 High frequency wireless power transfer system. The transmitter includes a high power radio frequency (RF) source with directional antenna. The implanted receiver unit includes a millimeter-size antenna with matching network and rectifier to convert the RF signal to DC voltage.

equivalent dimensions of the external coil with respect to the operating wavelength λ (speed of light in the medium/operating frequency), a significant amount of input power can be dissipated as radiated energy which does not couple with the implant coil. However, some designs have utilized directional antennas to focus the incident beam pattern at the implant site [28]. Due to its large operating distance and option of focused energy transfer, this technique was widely adopted for long range ultra-high frequency (UHF) RFID tags for keyless entry and resource management [29].

14.2.1.2.3 Permanent Magnet-Based Power Transfer Recently an alternative approach was proposed for generating a time-varying magnetic field using the rotation of permanent magnets [30]. In this approach, the energy was converted from stored chemical (battery) form to mechanical form, driving the motor. A high magnetic field intensity (75,000 A/m) permanent magnet, based on neodymium, iron, and boron (NdFeB) material, was connected to the motor. Figure 14.4 shows the block diagram of the system. With the rotation of the magnetic core, the magnetic field coupled to the receiver coil varied over time, resulting in an induced voltage at the implant. The operating frequency was limited to below 200 Hz due to the rotation speed of the motor (90 turns/second). It was argued that the low frequency operation led to significantly lower absorbed energy in the tissue, thus making this approach safer for biomedical applications. However, unintentional stimulation or modulation of the underlying neuronal network was not considered, which is critical

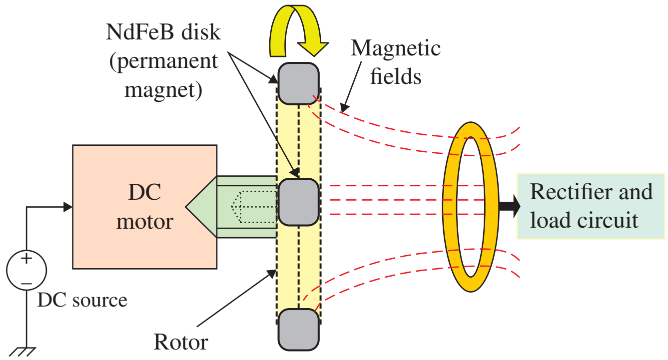

FIGURE 14.4 Permanent magnet-based wireless power transfer. The transmitter system includes high magnetic field intensity magnets positioned on the rotor. With the circular motion of the rotor, the coupled magnetic field in the receiver coils changes over time, which creates the voltage across the load circuit. Energy is converted from the electric form to mechanical form and back to electric form.

due to the low frequency temporal coding of neural signals. Much research is needed to address the safety and efficacy of this approach. For wearable electronics, this approach may not be useful due to the small operating range and total mass of the motor-based system.

14.2.1.3 Ultrasound Powered Source Ultrasound-based power transfer, from a dedicated energy source to a small-sized implanted or wearable system, is a novel technique. Compared to an electromagnetic field, acoustic waves travel many orders slower (velocity of acoustic wave/electromagnetic wave in air $\sim 10^{-6}$) inside the propagation mediums (i.e., air, tissue), which results in the acoustic signal having a small operating wavelength (1–2 mm) while operating at the MHz frequency range (typically called ultrasound). Instead of using direct or induced electric current for energy transfer, the ultrasound source creates pressure waves. These waves travel through the biological medium and are intercepted by the receiver which converts the acoustic energy back into electrical energy. Due to low losses of acoustic signals in biological tissue, implanted devices can be implanted deep inside the body (5–50 mm) [31,32]. Significant research has been dedicated to create focused ultrasound beams for the non-invasive imaging of soft tissues. Typically, piezoelectric transducers (PZT) were used to create acoustic signals [31]. However, due to high acoustic impedance of the PZT compared to air (acoustic impedance of PZT/acoustic impedance of air $\sim$75,000), it requires direct contact between the transducer and the tissue to reduce the impedance mismatch between different propagating mediums. During the use of PZT, matching layers were applied to the device, to match the acoustic impedance of the PZT (Z_{PZT} = 31 MRayl) to the tissue impedance (Z_{tissue} = 1.5 MRayl). Figure 14.5 shows a typical block diagram of ultrasound-based power transfer to the implanted device. The tissue attenuation coefficient α increases with the operating frequency f ($\alpha = 0.7f^{1.2}$ dB/cm) and a frequency range of 200 kHz to 1.2 MHz was

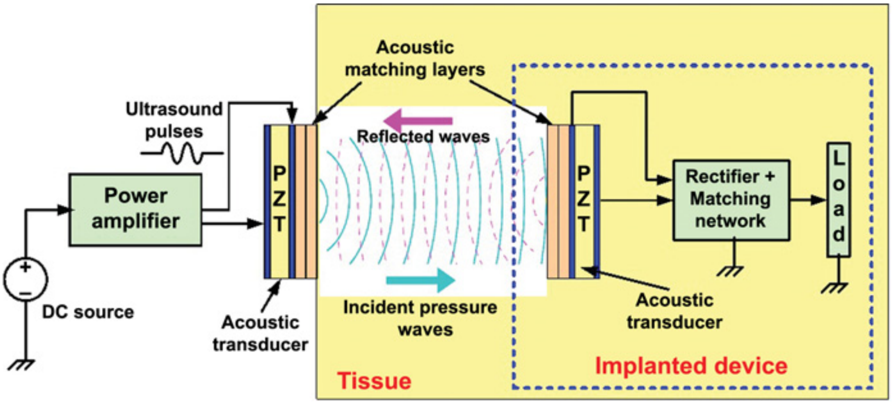

FIGURE 14.5 Ultrasound wireless power transfer system. The external source generates the ultrasound pressure waves which can travel through the tissue. The implanted acoustic transducer converts the acoustic energy to electric energy.

recommended for the ultrasound-based power transfer [31]. This design successfully transferred 70 mW of power to the deep implant (depth = 40 mm) with a power transfer efficiency of 27%.

14.2.1.4 Light Powered Source Recently, an incoherent light source was successfully used to transfer energy to an implant through tissue [33]. The design utilized a wearable near-infrared light emitting diode (LED)-based light source with a central wavelength of 850 nm (Figure 14.6). An implanted photo voltaic (PV) cell was used to convert the received photons to electric current. In the external unit, an LED source was used in combination with a parabolic reflector and a planoconvex lens to control the depth of focus inside the tissue. Due to the smaller penetration depth of the near-infrared signal compared to inductive or ultrasound sources, this method can only be used to charge or power shallow implants (depth of 5–10 mm). However, the abundance of incoherent light sources such as LEDs, makes this method a useful power transfer technique. For wearable devices, this technique can be exceptionally useful as there can be a direct path through the air between the light source and the receiver PV cell. As the near-infrared light propagates through the biological tissue, a significant amount of incident energy is absorbed, causing increased local tissue temperature. Therefore, a safety study of this technique needs to be considered before deciding on the input power of the light source.

14.2.2 Regenerative Energy Harvesting Devices

With the development of ultra-low power electronics such as micro- and nano-watt biosensors, it is now possible to power some of these systems directly through ambient energy. A significant amount of research was dedicated to convert abundant solar energy to useful electric energy. Similarly, some attempts were made at harvesting vibration and electromagnetic energy for device operation. Typically, these systems

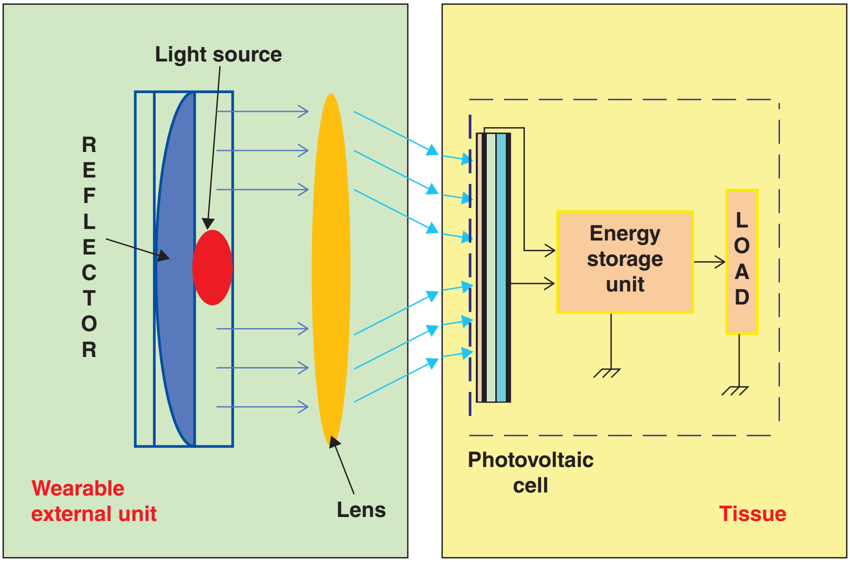

FIGURE 14.6 Light source-based wireless power transfer. The power source includes light source (LED), parabolic reflector, and convex lens to focus the light beam at the receive site. The implanted photovoltaic cell converts the light energy to electric form.

involve an energy harvester device which converts the ambient energy to electric current. In many cases, this energy is accumulated inside a storage unit (i.e., supercapacitor, battery) over the time span of a few seconds to hours, to meet the power requirement of the underlying application. In the following sections, different harvesting techniques are discussed.

14.2.2.1 Mechanical Energy Harvester Piezoelectric material is one of the leading devices that converts mechanical energy to electric form and vice versa. When an external pressure or force is applied across the piezoelectric material, the internal dipoles orient to create non-zero voltage across the terminals. In the presence of repetitive pressure at the resonance frequency of the piezoelectric structure, substantial mechanical energy can be converted to an electric signal. Depending on the vibration direction, different resonance modes (at separate frequencies) can be generated inside the material. Therefore, a single device can harvest energy from a wide frequency range of external vibrations [1, 8, 34–36]. In general, the human body generates multiple low frequency rhythmic signals (i.e., human heartbeats, respiratory action, and fluctuating blood pressure). Many voluntary actions such as walking and running can also create sufficient energy for low power wearable electronics [37]. So, some designs have proposed favorable energy harvesting locations (i.e., ankle, knee, hip, shoulder) for piezoelectric devices [36, 38, 39].

14.2.2.2 Photovoltaic Cell Since the discovery of the photoelectric effect, there has been a systematic effort to convert abundant solar energy (density ~1000 W/m^2)

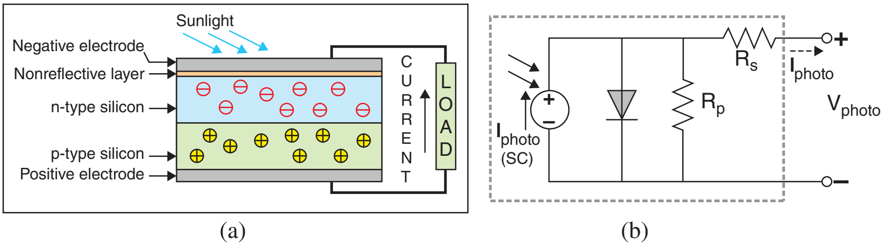

FIGURE 14.7 (a) Block diagram of a photovoltaic cell that converts solar energy to electrical energy. The PV cell uses n-type and p-type silicon layers and can be easily fabricated using standard micro-fabrication technology. (b) Norton equivalent of the PV cell. The photo-current ($I_{photo(SC)}$) is the current drawn from the cell at zero-load condition. V_{photo} is the open-circuit (infinite load) voltage across the PV cell.

to useful electric energy [40, 41]. Traditionally, the conversion efficiency (photonic energy to electrical energy) of solar (photovoltaic) cells has been below 10%. With advancements in microfabrication technologies that can create multi-junction cells, a peak power conversion efficiency of 44.7% has been achieved [42]. However, low cost and commercially available solar cells are still limited to efficiencies of 15–20% and can be useful to power only low or moderate power wearable devices. Figure 14.7 shows the block diagram of photovoltaic based energy harvesters. This technique can be very useful for powering wearable electronics such as health monitoring sensors. By including a tiny strip of solar cell (area = 1 cm^2), sufficient electric energy (~1–10 mW) can be generated and can be stored in the on-site batteries during daytime.

14.2.2.3 Electromagnetic Energy Harvester With the increasing connectivity of the wireless links (i.e., GSM, WiFi) to the mobile device, substantial electromagnetic energy can be present around us. Even if an individual wireless link is only short-lived and narrow band, the time-multiplexed operation of multiple devices results in a very low power broadband electromagnetic spectrum (~0.01–0.1 μW/cm^2). To demonstrate this, one study has created a prototype electromagnetic (EM) energy harvester system that captures EM signals over the global system for mobile (GSM) communication band (900 MHz, 1800 MHz) [43]. A similar approach was taken to harvest energy from 240 MHz to 710 MHz. The design used an active antenna based on a metamaterial split ring resonator (SRR) to achieve broadband impedance matching [11]. Typically, these designs require a broadband antenna, multistage voltage doubler, and high efficiency rectifier circuit to substantially enhance the input voltage across the antenna and rectify the signal as DC current to charge an energy storage unit (i.e., battery, super capacitor). Figure 14.8 shows the typical block diagram of an electromagnetic field-based energy transfer system.

14.2.2.4 Thermoelectric Substrate Thermoelectric generators (TEG) operate on the Seebeck effect, which states that in the presence of a temperature gradient in the TEG device, electric current can be generated and vice versa [37, 44]. In these devices, two thermocouples or thermojunctions are created by using two metals or alloys with

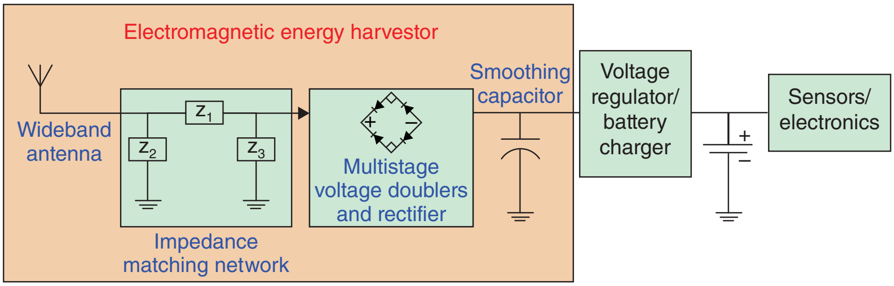

FIGURE 14.8 Block diagram of electromagnetic energy absorber. The module includes wide band antenna (i.e., spiral, log-periodic), matching network, multistage voltage doubler, and energy storage unit.

different Seebeck coefficients. When there is a temperature difference between these thermojunctions, an electric current flows in the device, which can be used to operate low power devices. Typically, p-doped and n-doped materials can be used as two materials to create a TEG device. In recent years, TEG devices have been found useful in powering implantable devices. The temperature of the human skin modulates with the ambient temperature. However, the internal temperature of the body is well regulated at 37°C. Therefore, a TEG device implanted near the skin surface experiences a temperature gradient between the two interfaces of the device. Depending on the thickness of the TEG device and its location, a substantial (1−2°C) temperature difference between the two interfaces (or thermojunctions) can be achieved. Such devices were successfully tested to power implanted electronics with power requirements of 10−100 μW [45,46]. Moreover, this technique can be useful to power wearable electronics as well. For example, recent research used a thermoelectric (TE) polymer coated over commercial fabric to create TE fabric suitable for harvesting body heat energy [47].

14.2.2.5 Biofuel Powered Devices In the field of bio-inspired electronics, using biofuel as an energy source has been long sought. The human body utilizes the binding energy of carbon-based molecules (i.e., sucrose, glucose) to perform bodily functions. Biofuel was considered in an attempt to mimic this process in self-powered implantable medical devices. The design converts chemical (or binding) energy of internal molecules, which are abundant and easily available through the food supply, to useful electrical energy. A functional glucose biofuel cell was proposed based on the wide variety of enzymes and redox mediators and was implanted inside a freely moving animal [48]. The design achieved peak power generation of 24.4 μW/mL which is sufficient to power low power sensors or neural stimulators (i.e., pacemaker).

14.3 DATA COMMUNICATION TO IMPLANTS AND WEARABLE SYSTEMS

Suitable operation of an implanted device depends on the individual patient and the device's operating conditions. Therefore, all implanted medical devices require a data communication channel between the external controller and the implanted device for remotely modifying the implant's parameters and/or to record internal biosignals. For any implanted device, specifications of the data channel depend on the required data rate, operating range, and its dimensions. Typically, each implanted device interacts with a dedicated external controller. Most device manufacturers use a different propriety communication protocol and operating frequency for the data link. However, in the age of wide data connectivity, recent designs have attempted to utilize industry standard protocols (i.e., Bluetooth Low Energy (BLE), MICS band) to achieve connection with the wireless network. In most designs, electromagnetic fields were created using a radio frequency source and were used effectively to transfer useful data between external and implanted systems. Some effort was dedicated to use an acoustic signal to achieve a low loss data link [31].

Wearable systems, in contrast, interact with a wide variety of devices. Therefore, these systems commonly adopted industry standard protocols (i.e., bluetooth, ZigBee, WiFi, ANT_{+}, NFC) while operating in the license free frequency bands. Selection of the individual standard depends on the required data rate, power budget for the communication, and the operating range. Depending on the underlying application and operating conditions, data communication channels are either low frequency (below 100 MHz) or high frequency (above 100 MHz). In the following sections, the differences between the different channels are discussed.

14.3.1 Low Frequency

Most implanted devices with a dedicated external controller operate over a short range and require few control instructions. For these devices, the dimensions of the implanted antenna needs to be small (below 1−2 cm) and the data communication channel needs to be reliable (low data packet loss). Due to low propagation loss (or attenuation) for low frequency (LF) signals inside the tissue, LF channels are commonly used for implanted medical devices (i.e., spinal cord stimulator, pacemaker, deep brain stimulator) [16, 17]. Using moderate size implant coils (1−2 cm diameter), a short operating range (1−5 cm) and a moderate data rate (100 kbps to 2 Mbps) was achieved for these designs [10].

Most implantable designs require both the wireless power and data link between the external and implanted system. In multiple designs, the power signal is modulated using the data signal, and control data from the external system is transferred over the power link. These designs are commonly referred to as single band power and data link. Typically, the absorbed energy (in the tissue) associated with the power carrier frequency is high and increases with the operating frequency. So, the associated data bandwidth is limited (500 kHz to 2 MHz) due to the use of a low power carrier frequency (below 10 MHz). To decouple this dependence, the dual band power and data link was proposed [10]. Using low frequencies (below 1 MHz) for the power transfer and moderate frequencies (10−50 MHz) for the data channel, data rates up to 1−2 Mbps were achieved without increasing the absorbed energy in the tissue [49]. Figure 14.9 shows the block diagram of single and dual band power and data transfer. To retrieve the status of the implant, an uplink channel (from the implant to the external) is required. Depending on the required data rate and implant complexity, the

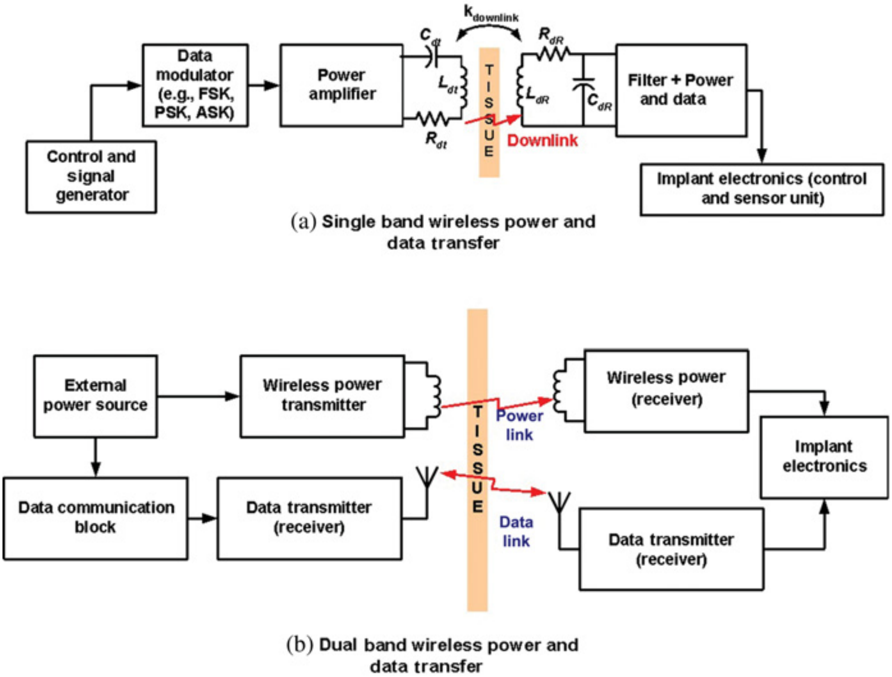

FIGURE 14.9 (a) Single band wireless power and data transfer. The data signal modulates the power signal in the form of amplitude, frequency, or phase. The achievable data rate for the single band system is limited by the carrier frequency of the power signal. (b) Dual band wireless and data transfer system. The power link uses a low frequency carrier to reduce energy absorption in tissue, while the data link utilizes the high frequency carrier to achieve a high data rate.

back telemetry system either uses a back scattering mechanism to deliver data over the power carrier signal [50] or uses a separate channel for the uplink communication.

For many wearable devices, the communication range between the reader and the wearable electronics is limited to few centimeters to achieve a secure data communication channel. For example, electronic wallets such as Google Wallet or Apply Pay use the in-built near field communication (NFC) system to achieve secure transactions. A similar approach was applied to RFID-based keyless entry or contactless access to health monitoring devices in a dense hospital environment.

14.3.2 High Frequency

High frequency data communication is commonly used for longer distances (1–10 m), high data rates (2–10 Mbps), and small implants. For these systems, the operating frequency is primarily limited to a few bands that can ensure no interference with commercial licensed bands. Depending on the region, some bands are kept license free for industrial, medical, and research usage. Table 14.1 provides

TABLE 14.1 Unlicensed frequency bands.

Frequency	Descriptions
433.05–434.79 MHz, 868–870 MHz	Europe unlicensed ISM bands
902–928 MHz	US unlicensed ISM band
2400–2483.5 MHz	Unlicensed ISM band (worldwide)
5150–5350 MHz, 5470–5825 MHz	ISM unlicensed (worldwide)
402–405 MHz	MICS band (worldwide)
401–406 MHz	MICS band extended (worldwide)
174–216 MHz, 470–608 MHz, 614–668 MHz	Wireless medical telemetry
608–614 MHz, 1395–1400 MHz, 1427–1432 MHz	WMTS bands (1.5 MHz/channel)
202.65–205.15 MHz	WMTS in New Zealand
420–429 MHz, 440–449 MHz	WMTS bands in Japan

a list of some dedicated bands operating in different regions of the world. Depending on the application, one or more frequency bands can be used. For example, the Industrial, Scientific, and Medical (ISM) band can be used for any medical and/or commercial applications. However, the Medical Implant Communications Service (MICS) band can only be used for communication with implanted devices. Since the MICS band shares the frequency spectrum with a licensed application, the transmitted power and data communication protocol is strictly regulated. The Wireless Medical Telemetry Service (WMTS) band can be used for any implantable and wearable medical devices. Due to worldwide license-free usage of the MICS (402−405 MHz) and ISM (2400−2483.5 MHz) bands, most medical, implanted, and wearable devices use antennas operating at these frequencies.

Typically, a communication network created by wearable or implanted devices is referred to as a BAN (Figure 14.10) [51, 52]. Significant research was contributed to characterize the proportion channel between different sensor nodes [9, 53]. To achieve the large-scale, secured network connectivity for implanted and wearable devices, different communication protocols were developed. Bluetooth, Zigbee, and ANT_+ are some of the dominant communication protocols operating in the high frequency ISM band (2400−2483.5 MHz). For a wearable or implanted device, selection of individual protocols was determined based on the power budget, network size (number of nodes), data rate, and operating distance.

14.4 DISCUSSION

In the last decade, with the rapid advancements in micro- and nano-fabrication technology, low power, small dimension and multifunctional implants and wearable electronics were developed. While on-site batteries served as the common source of power for computationally intensive devices (i.e., smart watch), the new contactless power delivery methods (i.e., ultrasound, inductive) were employed on medical implants to achieve longevity and smaller device dimensions. For these designs, trade-offs were made between the dimensions, mass, and replacement/rechargeable period of the energy source. To achieve batteryless and life-long operation of the system, energy harvesting methods were proposed, which can convert ambient

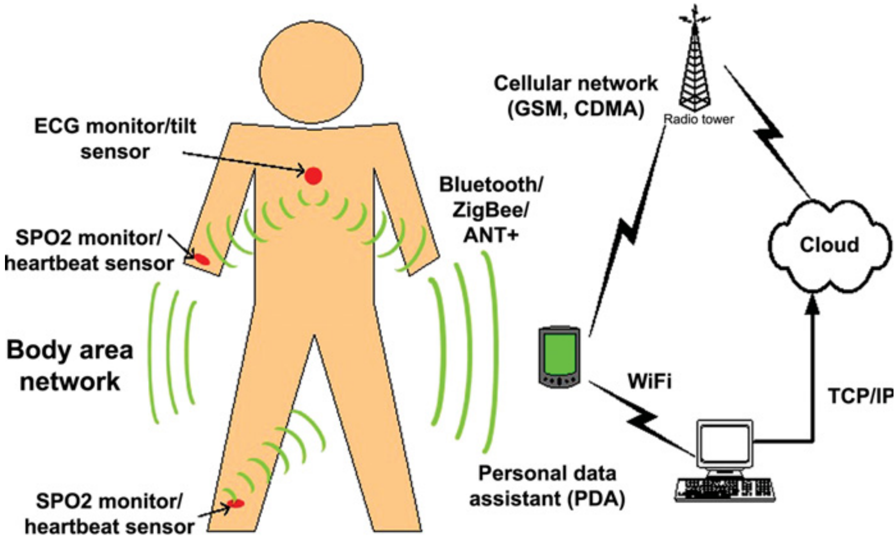

FIGURE 14.10 Block diagram of the typical body area network (BAN). The system includes the body-worn sensors/electronics with the capability of radio communication. The multi-node sensor network can communicate over the standard protocols such as Bluetooth, ZigBee and ANT_+. The range of the BAN can be extended by interfacing with the cellular or wired network.

mechanical, electromagnetic, solar, and/or chemical energy to useful electrical energy. Current energy harvesting technologies are limited to very low power (micro- and nano-watt) devices. However, further increases in the energy conversion efficiency (between ambient and electrical forms) will lead to self-powered and sustained energy sources for wearable and implanted electronics.

The specifications (frequency and data rate) of the communication channels vary across the different applications. Most implanted devices use application specific and proprietary communication links, which can be operated over a short range (less than 5 cm). However, with the desire for long-term implant monitoring and remote connectivity, new implants are equipped with high frequency radiofrequency (RF) transceivers. To communicate with the implanted system over large distances (2−10 m), the MICS band (402−405 MHz) was adopted, due to its worldwide usage and low attenuation compared to the ISM band (2400−2483.5 MHz). For on-body wearable electronics, the high frequency ISM band was utilized to create a multi-node network between the on-body sensors and the surrounding network. Table 14.2 provides the design selection and its limitations to effectively deliver power and data to implantable/wearable electronics.

14.5 DESIGN EXAMPLES

14.5.1 Wireless Power and Data for Retinal Prosthesis

The retinal prosthesis is one of the most successful medical devices that restores partial vision in patients with age-related macular degeneration (AMD) and retinitis

TABLE 14.2 Comparison between different power mechanism.

Non-regenerative power source	Mechanism	Power range	Primary application
On-site battery [3, 17]	Direct DC source	100mW–2 W	Wearable, implants
Wireless power [22]	Electromagnetic field coupling	1–50 mW	Implants (i.e., retinal prosthesis)
Ultrasound [31]	High frequency pressure wave	1–50 mW	Deep tissue implants
Optical [33]	Near-infrared light	1–20 mW	Wearable sensors, implants
Regenerative power source	Mechanism	Power range	Primary application
Mechanical [37]	Vibration, pressure	0.01–0.1 mW	Wearable sensors
Solar cell [40]	Photoelectric	0.1–10 mW	Wearable sensors
Electromagnetic field harvester [11]	High frequency (HF) field absorber	0.01–1 mW	Wearable sensors
Thermoelectric [46]	Seebeck effect	0.01–0.1 mW	Wearable sensors, shallow implants
Biofuel [48]	Chemical reaction	0.01–1 mW	Deep body implants

pigmentosa (RP) [4]. Figure 14.11 shows the block diagram of the retinal prosthesis system which uses a hybrid design of implanted and wearable electronics. The battery operated body-worn processing unit transfers energy and data to the implanted electronics to create visual perceptions. It uses epiretinal electrodes to bypass the defective photoreceptors and electrically stimulate retinal ganglion to generate neural activities. The visual perception of the patient depends on the spatial and temporal distribution of the stimulation pattern. Therefore, a body-worn processing unit is used to generate an optimal stimulating pattern based on the surroundings. In this design, an eyeglasses-mounted camera captures external images and a body-worn unit performs real-time processing on the images to generate stimulation patterns.

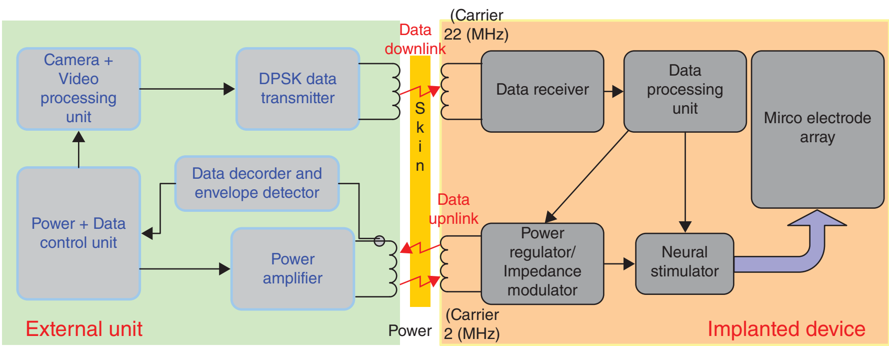

FIGURE 14.11 Block diagram of retinal prosthesis system based on the design proposed in [49]. *Source:* Chen et al. 2010 [49]. Reproduced with permission of IEEE.

Due to the complexity and energy requirement of the image processor, all the computation is performed outside the body while keeping the basic function of the implanted neural stimulator. Due to a large multi-electrode array being necessary for generating high resolution visual perception, the power requirement of the implant can vary largely from 50 mW to 250 mW [49]. In this design, an external power source (battery) is used and energy is transferred wirelessly (using low frequency inductive coupling) to the small-sized implant. Typically, such WPT systems achieve a total efficiency of 10–15%. Therefore, a small form factor rechargeable battery was used to achieve a time period of 4–6 hours between individual charging cycles [54]. To control the stimulation pattern, the design uses the forward telemetry link (downlink) modulated (amplitude modulation) over the power signal. During device operation, the eye can rotate, which may result in a temporary loss of power link. Therefore, a back telemetry link (uplink) is used to create a feedback loop that can result in constant output power at the implant.

14.5.2 Wireless Sensors for the Body Area Network

With the development of small and power-efficient health monitoring sensors, multiple applications have attempted to create a local and secure BAN around individuals [53]. Medtronic's data connectivity solutions is one of the leading patient management systems which helps with connecting an implanted cardiac device to a clinical system. Figure 14.12 provides the schematics of the patient management system. Some designs utilize sensor modules that can be scaled to create a network formation. For these designs, low weight, small form factor, and improved battery life are the key design requirements. To create a multi-node network, these devices use radio frequency (RF) transceivers while operating at standard communication protocols to achieve seamless compatibility with other devices. The high frequency

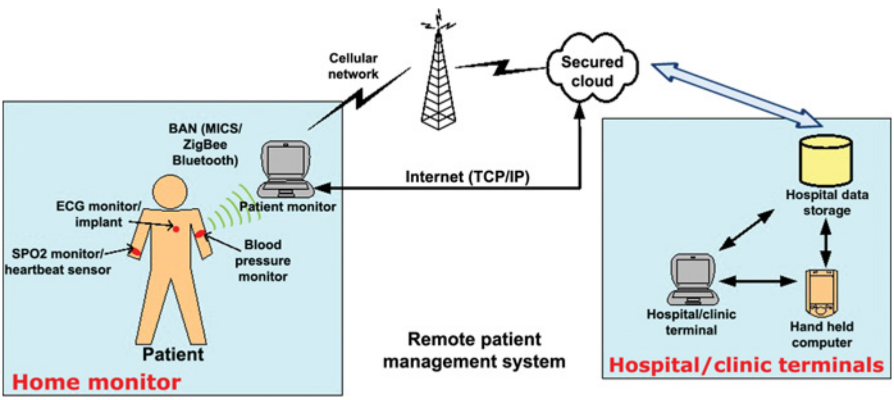

FIGURE 14.12 Block diagram of the remote patient management system. The home monitor can wirelessly track the vital signs of the patient and communicate the relevant information in real time or periodically to the secured server of the hospital. Physicians can access these records to make decisions on the patient's health.

ISM band (2400−2483.5 MHz) is a commonly used unlicensed band (worldwide) for the BAN. Due to wide usage of this spectrum, different form factors of antennas were proposed that can fit inside wearable device to create the desired radiation pattern. Patch antennas, inverted-F, monopoles, and meanders are commonly used antennas for wearable electronics. In some designs, novel antenna fabrication techniques were used in which antennas can be embedded inside the user's clothing or can be mounted as a flexible bandage. Independent of the antenna selection, multiple communication protocols such as WiFi, Bluetooth, BLE, ANT_+, ZigBee can be operated over the ISM spectrum. For different applications, selection among individual protocols is determined based on the required data rate, number of network nodes, power budget of the device and added license cost for the use of protocol. Bluetooth and WiFi can support high data rates (1−54 Mbps) at the expense of higher power requirements. Low energy Bluetooth devices transfer device status information in the form of small packets 8−27 bytes and require a fraction of the power compared to Bluetooth High Speed(HS). ANT_+ is a proprietary protocol which is used for sensor networks and remote control systems. Some applications include access to heart rate monitors, cycling power meter monitors, and control of music players.

14.6 CONCLUSION

The need for energy efficient and multi-functional implanted or wearable devices has driven research into novel power and data telemetry techniques. While batteries have remained the primary energy source for such devices, multiple efficient and safe WPT methods were developed to reduce the size of implants. To improve the longevity of the wearable and implanted devices, energy harvesting devices were proposed which can convert ambient energy (i.e., solar, vibration, pressure, electromagnetic, biofuel) into useful electric energy. Currently, such harvesting devices are limited to powering low power (0.1−10 mW) electronics. However, with the improvement of energy harvesting efficiency, such methods can be widely applied in conjunction with traditional powering mechanisms (i.e., battery).

Most wearable electronics and implanted devices are equipped with radio frequency transceivers. The specifications of the data link (operating frequency, data rate, protocol) differ in different systems. Most of the current implanted devices use a dedicated controller without the option of network connectivity. However, in the era of the Internet of Things and Big Data, some research is being undertaken to retrieve device status and capture a patient's long-term biosensor data over a secure network. Such studies can significantly benefit the medical community by improving system efficiency and allowing individuals to track their fitness.

REFERENCES

[1] A. Fowler, S. Moheimani, and S. Behrens, "A 3-DOF SOI MEMS ultrasonic energy harvester for implanted devices," *J. Phys.: Conf. Ser.*, *PowerMEMS 2013,* vol. 476, pp. 1–5, 2013.

[2] W. Burleson, S. S. Clark, B. Ransford, and K. Fu, "Design Challenges for Secure Implantable Medical Devices," in Proceedings of the 49th Annual Design Automation Conference, ACM, 2012, pp. 12–17.

[3] D. Cooper, The Wearables Industry Needs to Brace Itself for the Apple Watch, 2015. Available at http://www.engadget.com/2015/03/09/wearables-industry-apple-watch/

[4] Second Sight, How is Argus II Designed to Produce Sight? 2014. Available at http://www.engadget.com/2015/03/09/wearables-industry-apple-watch/

[5] J. Paulo and P. Gaspar, "Review and Future Trend of Energy Harvesting Methods for Portable Medical Devices," in Proceedings of the World Congress on Engineering 2010 Vol II, June 30–July 2, London, 2010.

[6] Daniel Burrus, Google Glass is Transforming Wearable Technology, 2014. Available at http://www.huffingtonpost.com/daniel-burrus/google-glass-is-transform b 4949991 .html

[7] Wearable Technology Life, Wearable Technology Life, 2015. Available at http://www.wearabletechnologylife.com/fitbit/

[8] K. Cook-Chennault, N. Thambi, and A. Sastry, "Powering mems portable devices: a review of non-regenerative and regenerative power supply systems with special emphasis on piezoelectric energy harvesting systems," *Smart Mater. Struct.*, vol. 17, no. 4, pp. 043001–043033, 2008.

[9] J. Abouei, J. D. Brown, K. N. Plataniotis, and S. Pasupathy, "Energy efficiency and reliability in wireless biomedical implant systems," *IEEE Trans. Information Technol. Biomed.*, vol. 15, no. 3, pp. 456–466, 2011.

[10] G. Wang, W. Liu, M. Sivaprakasam, and G. A. Kendir, "Design and analysis of an adaptive transcutaneous power telemetry for biomedical implants," *IEEE Trans. Circuits Syst. I: Regular Papers*, vol. 52, no. 10, pp. 2109–2117, October 2005.

[11] G. Fu and S. Sonkusale, "Broadband energy harvesting using a metamaterial resonator embedded with non-foster impedance circuitry," *arXiv preprint arXiv*:1411.0662, 2014.

[12] E. Y. Chow, C.-L. Yang, Y. Ouyang, A. L. Chlebowski, P. P. Irazoqui, and W. J. Chappell, "Wireless powering and the study of RF propagation through ocular tissue for development of implantable sensors," *IEEE Trans. Antennas Propag.*, vol. 59, no. 6, pp. 2379–2387, April 2011.

[13] A. V. Nurmikko, J. P. Donoghue, L. R. Hochberg, W. R. Patterson, Y.-K. Song, C. W. Bull, D. A. Borton, F. Laiwalla, S. Park, Y. Ming, and J. Aceros, "Listening to brain microcircuits for interfacing with external world—progress in wireless implantable microelectronic neuroengineering devices," *Proc. IEEE*, vol. 98, no. 3, pp. 375–388, February 2010.

[14] M. Koo, K.-I. Park, S. H. Lee, M. Suh, D. Y. Jeon, J. W. Choi, K. Kang, and K. J. Lee, "Bendable inorganic thin-film battery for fully flexible electronic systems," *Nano Lett.*, vol. 12, no. 9, pp. 4810–4816, July 2012.

[15] L. Hu, H. Wu, F. La Mantia, Y. Yang, and Y. Cui, "Thin, flexible secondary Li-ion paper batteries," *ACS Nano.*, vol. 4, no. 10, pp. 5843–5848, October 2010.

[16] Boston Scientific Inc., Spinal Cord Stimulator Systems, 2015. Available at http://www.bostonscientific.com/en-US/products/spinal-cord-stimulator-systems.html

[17] Medtronic Inc., Bradycardia, 2015. Available at http://www.medtronic.com/patients/bradycardia/pacemaker/

[18] A. Qusba, A. RamRakhyani, J.-H. So, G. Hayes, M. Dickey, and G. Lazzi, “On the design of microfluidic implant coil for flexible telemetry system,” *IEEE Sens. J.*, vol. 14, no. 4, pp. 1074–1080, April 2014.

[19] A. RamRakhyani, S. Mirabbasi, and M. Chiao, “Design and optimization of resonance-based efficient wireless power delivery systems for biomedical implants,” *IEEE Trans. Biomed. Circuits Syst.*, vol. 5, no. 1, pp. 48–63, February 2011.

[20] V. Singh, A. Qusba, A. Roy, R. Castro, K. McClure, R. Dai, R. Greenberg, J. Weiland, M. Humayun, and G. Lazzi, “Specific absorption rate and current densities in the human eye and head induced by the telemetry link of an epiretinal prosthesis,” *IEEE Trans. Antennas Propag.*, vol. 57, no. 10, pp. 3110–3118, October 2009.

[21] L. Wu, Z. Yang, E. Basham, and W. Liu, “An Efficient Wireless Power Link for High Voltage Retinal Implant,” in 2008 IEEE Conference on Biomedical Circuits and Systems, BioCAS 2008, Baltimore, November 20–22, 2008, pp. 101–104.

[22] A. K. RamRakhyani and G. Lazzi, “On the design of efficient multi-coil telemetry system for biomedical implants,” *IEEE Trans. Biomed. Circuits Syst.*, vol. 7, no. 1, pp. 11–23, 2013.

[23] A. RamRakhyani and G. Lazzi, “Use of Multi-Coil Telemetry System for High Tolerance Efficient Wireless Power System,” in 2012 IEEE International Conference on Wireless Information Technology and Systems (ICWITS), Maui, HI, November11–16, 2012, pp. 1–4.

[24] A. RamRakhyani and G. Lazzi, “Multi-coil approach to reduce electromagnetic energy absorption for wireless powered implants,” *IET Healthc. Technol. Lett.*, March 2014, pp. 21–25.

[25] A. RamRakhyani and G. Lazzi, “Interference-free wireless power transfer system for biomedical implants using multicoil approach,” *Electron. Lett.*, vol. 50, no. 12, pp. 853–855, June 2014.

[26] D. Pivonka, A. Yakovlev, A. Poon, and T. Meng, “A mm-sized wirelessly powered and remotely controlled locomotive implant,” *IEEE Trans. Biomed. Circuits Syst.*, vol. 6, no. 6, pp. 523–532, December 2012.

[27] A. Ma and A. Poon, “Midfield wireless power transfer for bioelectronics,” *IEEE Circuits and Syst. Mag.*, vol. 15, no. 2, pp. 54–60, Secondquarter 2015.

[28] G. Yang, M. R. Islam, R. A. Dougal, and M. Ali, “A reconfigurable stacked patch antenna for wireless power transfer and data telemetry in sensors,” *Prog. Electromagnetics Res.*, vol. 29, pp. 67–81, Secondquarter 2012.

[29] P. Nikitin, K. Rao, and S. Lazar, “An Overview of Near Field UHF RFID,” in 2007 IEEE International Conference on RFID, Grapevine, TX, March 26–28, 2007, pp. 167–174.

[30] H. Jiang, J. Zhang, D. Lan, K. K. Chao, S. Liou, H. Shahnasser, R. Fechter, S. Hirose, M. Harrison, and S. Roy, “A low-frequency versatile wireless power transfer technology for biomedical implants,” *IEEE Trans. Biomed. Circuits Syst.*, vol. 7, no. 4, pp. 526–535, 2013.

[31] S. Ozeri and D. Shmilovitz, “Ultrasonic transcutaneous energy transfer for powering implanted devices,” *Ultrason.*, vol. 50, no. 6, pp. 556–566, 2010.

[32] H. Vihvelin, J. Leadbetter, M. Bance, J. A. Brown, and R. B. Adamson, “Compensating for tissue changes in an ultrasonic power link for implanted medical devices,” *IEEE Trans. Biomed. Circuits Syst.*, vol. 10, no. 2, pp. 404–411, April 2016.

[33] Y. Song, Q. Hao, X. Kong, L. Hu, J. Cao, and T. Gao, "Simulation of the recharging method of implantable biosensors based on a wearable incoherent light source," *Sensors*, vol. 14, no. 11, pp. 20687–20701, 2014.

[34] S. R. Anton, "Multifunctional Piezoelectric Energy Harvesting Concepts," Ph.D. Dissertation, Virginia Polytechnic Institute and State University, 2011.

[35] A. Fowler, S. Moheimani, and S. Behrens, "An omnidirectional mems ultrasonic energy harvester for implanted devices," *J. Microelectromech. Syst.*, vol. 23, no. 6, pp. 1454–1462, December 2014.

[36] C. Dagdeviren, B. D. Yang, Y. Su, P. L. Tran, P. Joe, E. Anderson, J. Xia, V. Doraiswamy, B. Dehdashti, X. Feng, L. et al., "Conformal piezoelectric energy harvesting and storage from motions of the heart, lung, and diaphragm," *Proc. Nati. Acad. Sci.*, vol. 111, no. 5, pp. 1927–1932, 2014.

[37] A. Cadei, A. Dionisi, E. Sardini, and M. Serpelloni, "Kinetic and thermal energy harvesters for implantable medical devices and biomedical autonomous sensors," *Meas. Sci. Technol.*, vol. 25, no. 1, pp. 012003–0120016, 2014.

[38] E. Romero, R. O. Warrington, and M. R. Neuman, "Body motion for powering biomedical devices," in, *Conf. Proc. IEEE Eng. Med. Biol. Soc.,* pp. 2752–2755, 2009.

[39] T. Starner, "Human-powered wearable computing," *IBM syst. J.*, vol. 35, no. 3-4, pp. 618–629, 1996.

[40] J. P. Carmo, J. M. Gomes, L. M. Goncalves, and J. H. Correia, "A flexible thin-film for powering stand-alone electronic devices," *Measurement*, vol. 46, no. 10, pp. 4145–4151, 2013.

[41] Z. L. Wang and W. Wu, "Nanotechnology-enabled energy harvesting for self-powered micro-/nanosystems," *Angew. Chem. Int. Ed.*, vol. 51, no. 47, pp. 11700–11721, 2012.

[42] F. Dimroth, M. Grave, P. Beutel, U. Fiedeler, C. Karcher, T. N. D. Tibbits, E. Oliva, G. Siefer, M. Schachtner, A. Wekkeli, A. W. Bett, R. Krause, M. Piccin, N. Blanc, C. Drazek, E. Guiot, B. Ghyselen, T. Salvetat, A. Tauzin, T. Signamarcheix, A. Dobrich, T. Hannappel, and K. Schwarzburg, "Wafer bonded four-junction gainp/gaas/gainasp/gainas concentrator solar cells with 44.7% efficiency," *Prog. Photovoltaics: Res. Appl.*, vol. 22, no. 3, pp. 277–282, 2014.

[43] L. M. Borges, R. Chavez-Santiago, N. Barroca, F. J. Velez, and I. Balasingham, "Radiofrequency energy harvesting for wearable sensors," *IET Healthc. Technol. Lett.*, vol. 2, no. 1, pp. 22–27, 2015.

[44] H. Bottner, "Thermoelectric Micro Devices: Current State, Recent Developments and Future Aspects for Technological Progress and Applications," in Proceedings of the Twenty-First International Conference on Thermoelectrics, ICT '02, August 25–29, 2002, pp. 511–518.

[45] M. Wahbah, M. Alhawari, B. Mohammad, H. Saleh, and M. Ismail, "Characterization of human body-based thermal and vibration energy harvesting for wearable devices," *IEEE J. Emer. Sel. Top. Circuits Syst.*, vol. 4, no. 3, pp. 354–363, September 2014.

[46] Y. Yang, X.-J.Wei, and J. Liu, "Suitability of a thermoelectric power generator for implantable medical electronic devices," *J. Phys. D: Appl. Phys.*, vol. 40, no. 18, pp. 5790, 2007.

[47] Y. Du, K. Cai, S. Chen, H. Wang, S. Shen, R. Donelson, and T. Lin, "Thermoelectric fabrics: toward power generating clothing," *Sci. Rep.*, vol. 4, April 2014.

[48] P. Cinquin, C. Gondran, F. Giroud, S. Mazabrard, A. Pellissier, F. Boucher, J.-P. Alcaraz, K. Gorgy, F. Lenouvel, S. Mathé, P. Porcu, and S. Cosnier, "A glucose biofuel cell implanted in rats," *PLoS One*, vol. 5, no. 5, pp. e10476, May 2010.

[49] K. Chen, Z. Yang, L. Hoang, J.Weiland, M. Humayun, and W. Liu, "An integrated 256-channel epiretinal prosthesis," *IEEE J. Solid-State Circuits*, vol. 45, no. 9, pp. 1946–1956, September 2010.

[50] M. Suster, J. Guo, N. Chaimanonart, W. Ko, and D. Young, "A Wireless Strain Sensing Microsystem With External RF Power Source and Two-Channel Data Telemetry Capability," in 2007 IEEE International Digest of Solid-State Circuits Conference, San Francisco, CA, February 11–15, 2007, pp. 380–609.

[51] A. Bindra, "Medical info-communications signals an era of body area networking," *RF Design*, pp. 10–14, February 2008.

[52] S. K. Kumar, "Design of a Wireless Platform for Wearable and Home Automation Applications," Ph.D. Dissertation, University of Missouri–Kansas City, 2012.

[53] D. Raskovic, T. Martin, and E. Jovanov, "Medical monitoring applications for wearable computing," *Comput. J.*, vol. 47, no. 4, pp. 495–504, 2004.

[54] Second Sight, Argus II Retinal Prosthesis System, 2015. Available at http://www.fda.gov/ucm/groups/fdagov-public/@fdagov-afda-adcom/documents/document/ucm320423.pdf